Reversible Symmetric Non-Expansive Convolution: An Effective Image Boundary Processing for M-Channel Lifting-based Linear-Phase Filter Banks

Taizo Suzuki, *Member, IEEE* and Masaaki Ikehara, *Senior Member, IEEE*

***Abstract*—We present an effective image boundary processing for M-channel ($M \in \mathbb{N}$, $M \geq 2$) lifting-based linear-phase filter banks (L-LPFBs) that are applied to unified lossy and lossless image compression (coding), i.e., lossy-to-lossless image coding. The reversible symmetric extension (RevSE) we propose is achieved by manipulating building blocks on the image boundary and reawakening the *symmetry* of "each building block" that has been lost due to rounding error on each lifting step. Moreover, complexity is reduced by extending non-expansive convolution, called reversible symmetric non-expansive convolution (RevSNEC), because the number of input signals does not even temporarily increase. Our method not only achieves reversible boundary processing, but also is comparable to irreversible SE (IrrSE) in lossy image coding and outperformed periodic extension (PE) in lossy-to-lossless image coding.**

***Index Terms*—Lifting-based linear-phase filter bank (L-LPFB), lossy-to-lossless image coding, reversible symmetric extension (RevSE), reversible symmetric non-expansive convolution (RevSNEC).**

I. Introduction

Filter banks (FBs) [1] have been contributing to signal processing and communication tools for many years. They have often been employed as transforms in image compression (coding) because they have extensive frequency selectivity and high coding gain. FBs with linear-phase (LP) properties, i.e., LPFBs [2–8], including lapped transforms (LTs) [9–14] are particularly one of the most useful transforms for image coding. LPFBs can be easily designed and they simply overcome problems with image boundary distortion via symmetric extension (SE) [2] that maintain continuity at the image boundary. The output signals can be reconstructed without image boundary distortion by using *symmetry* even if the extended signals are not transmitted to the synthesis bank. *Symmetry* means that when an input signal vector for a building block is the reflected vector of another input signal vector, their output signal vectors also have the same relationship. Smith and Eddins [2] achieved such SE by using the *symmetry* of "whole FB."

Lifting structures with rounding operations have also been presented [15–17]. A transform only composed of lifting structures and integer multipliers achieves an integer-to-integer transform that maps integer input signals to integer output signals. Thus, many lifting-based FBs (L-FBs) [18–23] including lifting-based LTs [24–26] have been proposed, and the structures have led FBs to achieve lossy-to-lossless image coding, which is unified lossy and lossless image coding, such as JPEG 2000 [27] and JPEG XR [28]. Discrete wavelet transforms (DWTs) [17] in JPEG 2000 have demonstrated excellent coding, whereas L-FBs have greater potential for lossy-to-lossless image coding due to their higher degrees of design freedom than DWTs. Several reversible smooth extensions have in fact been applied to 2-channel L-FBs including DWTs [21], [22], [29]. However, no smooth boundary extensions can directly be applied to generalized M-channel ($M \in \mathbb{N}$, $M \geq 2$) L-FBs. 4×8 hierarchical lapped transform (HLT) [30] in JPEG XR is well-known as one of the most popular L-FBs. Although it uses a constrained case of the image boundary solution we propose later, $M \times 2M$ L-LPFB case, it causes a little bit boundary error because SE cannot be precisely achieved by ignoring the scaling coefficients. Periodic extension (PE), which causes image boundary distortion, is often reluctantly used for lossy-to-lossless image coding based on M-channel L-FBs even if it has LP properties because rounding error on each lifting step corrupt *symmetry* [26].

We solve the image boundary problem in lossy-to-lossless image coding based on M-channel lifting-based LPFBs (L-LPFBs) by focusing on the *symmetry* of "each building block" unlike that of the "whole FB" [2]. Although the proposed reversible SE (RevSE) is not completely equivalent to SE, which is called irreversible SE (IrrSE) to distinguish it from RevSE, it can obtain very similar smoothness to IrrSE at the image boundary even if rounding operations are used. Moreover, complexity is reduced by extending non-expansive convolution [13], called reversible symmetric non-expansive convolution (RevSNEC), because the number of input signals does not even temporarily increase. The proposed RevSNEC can be applied to $M \times MK$ ($K \in \mathbb{N}$, $K \neq 0$, and K must only be odd in odd channel case) L-LPFBs which are extensions of $M \times 2M$ L-LPFBs as HLT in JPEG XR. The RevSNEC not only achieves reversible boundary processing, but also is comparable to IrrSE in lossy image coding and outperformed PE in lossy-to-lossless image coding.

The remaining part of this paper is organized as follows: Sec. II reviews the lattice structures of LPFBs and explains how we derive their lifting structures. Sec. III presents IrrSE using *symmetry* of "each building block" newly in both even and odd channel cases. This structures are extended to RevSE and RevSNEC by simple matrix manipulations. Filter design examples, lossy-to-lossless image coding simulations, and comparisons to the conventional methods are presented in Sec. IV. Sec. V concludes the paper.

Boldface letters represent vectors or matrices. $\mathbf{I}_N$, $\mathbf{J}_N$, $\mathbf{0}$, $\cdot^T$, $\mathrm{diag}(\cdots)$, and $\det(\cdot)$ respectively denote an $N \times N$ ($N \in \mathbb{N}$, $N \neq 0$) identity matrix, $N \times N$ reversal identity matrix, null matrix, transpose of a matrix, block diagonal matrix, and determinant of a matrix.

II. Lattice and Lifting Structures of LPFBs

A. Linear-Phase Filter Banks (LPFBs)

When $m \in \mathbb{N}$, $m \neq 0$, $M = 2m$ (M is even) and $M = 2m+1$ (M is odd), the type-II analysis polyphase matrix $\mathbf{E}(z)$ in $M \times MK$ LPFBs are presented as in Tran [6]:

$$\mathbf{E}(z) = \mathbf{E}_0 \mathbf{G}_1(z) \cdots \mathbf{G}_{K-2}(z) \mathbf{G}_{K-1}(z) \tag{1}$$

where

$$\mathbf{E}_0 = \mathbf{\Phi}_0 \mathbf{W}, \ \mathbf{G}_k(z) = \mathbf{\Lambda}(z) \mathbf{W} \mathbf{\Phi}_k \mathbf{W},$$

$$\mathbf{\Phi}_k = \begin{cases} \mathrm{diag}\{\mathbf{U}_{e,k}, \mathbf{V}_{e,k}\} & (M \text{ is even}) \\ \mathrm{diag}\{\mathbf{U}_{o,k}, \mathbf{V}_{o,k}\} & (M \text{ is odd, } k \text{ is even}) \\ \mathrm{diag}\{\mathbf{U}_{o,k}, w_k, \mathbf{V}_{o,k}\} & (M \text{ is odd, } k \text{ is odd}), \end{cases}$$

$$\mathbf{\Lambda}(z) = \begin{cases} \mathrm{diag}\{\mathbf{I}_m, z^{-1}\mathbf{I}_m\} & (M \text{ is even}) \\ \mathrm{diag}\{\mathbf{I}_{m+1}, z^{-1}\mathbf{I}_m\} & (M \text{ is odd}), \end{cases}$$

$$\mathbf{W} = \begin{cases} \frac{1}{\sqrt{2}} \begin{bmatrix} \mathbf{I}_m & \mathbf{J}_m \\ \mathbf{J}_m & -\mathbf{I}_m \end{bmatrix} & (M \text{ is even}) \\ \frac{1}{\sqrt{2}} \begin{bmatrix} \mathbf{I}_m & \mathbf{0} & \mathbf{J}_m \\ \mathbf{0} & \sqrt{2} & \mathbf{0} \\ \mathbf{J}_m & \mathbf{0} & -\mathbf{I}_m \end{bmatrix} & (M \text{ is odd}), \end{cases}$$

$\mathbf{U}_{e,k}$, $\mathbf{V}_{e,k}$, and $\mathbf{V}_{o,k}$ are $m \times m$ arbitrary nonsingular matrices, $\mathbf{U}_{o,k}$ is an $(m+1) \times (m+1)$ or $m \times m$ arbitrary nonsingular matrix

T. Suzuki is with the Faculty of Engineering, Information and Systems, University of Tsukuba, Tsukuba, Ibaraki, 305-8573 Japan (e-mail: taizo@cs.tsukuba.ac.jp).

M. Ikehara is with the Department of Electronics and Electrical Engineering, Keio University, Yokohama, Kanagawa, 223-8522 Japan (e-mail: ikehara@tkhm.elec.keio.ac.jp).

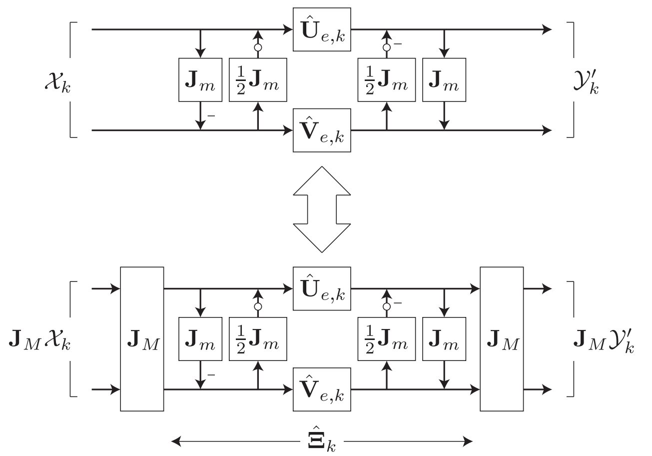

Fig. 1. Building blocks of M-channel L-LPFB in even channel case (white circles mean rounding operations, bold arrows mean $m \times 1$ vector signals, and narrow arrows mean scalar signals).

when k is even or odd, and w_k is a nonzero scalar. Also, either $\mathbf{U}_{e,k}$ or $\mathbf{V}_{e,k}$ and $\mathbf{V}_{o,k}$ are usually replaced by $\mathbf{I}_m$ when $k \geq 1$ to eliminate redundancy. If $\mathbf{E}(z)$ is invertible, synthesis polyphase matrix $\mathbf{R}(z)$ can be chosen as the inverse of $\mathbf{E}(z)$, i.e., the perfect reconstruction (PR) property $\mathbf{R}(z)\mathbf{E}(z) = \mathbf{I}_M$ is satisfied. The LPFBs are paraunitary LPFBs (PULPFBs) if all $\mathbf{U}_{e,k}$, $\mathbf{V}_{e,k}$, $\mathbf{U}_{o,k}$, and $\mathbf{V}_{o,k}$ are orthogonal matrices and w_k is 1, and the others are biorthogonal LPFBs (BOLPFBs). In PULPFBs, m must be $m \geq 2$. As described in Sec. III-A, IrrSE can simply be applied to the LPFBs to improve coding performance.

B. *Lifting-based Linear-Phase Filter Banks (L-LPFBs)*

This subsection presents L-LPFBs based on the polyphase matrix in Eq. (1). When all lifting steps are implemented with rounding operations, L-LPFBs achieve integer-to-integer mapping, i.e., the lossless mode. The building block $\mathbf{G}_k(z)$ in Eq. (1) to achieve this is represented as

$$\mathbf{G}_k(z) = \mathbf{\Lambda}(z)\mathbf{W}\mathbf{\Phi}_k\mathbf{W} = \mathbf{\Lambda}(z)\mathbf{W}_L\mathbf{\Phi}_k\mathbf{W}_R \triangleq \mathbf{\Lambda}(z)\mathbf{\Xi}_k$$

where

$$\mathbf{W}_L = \begin{cases} \begin{bmatrix} \mathbf{I}_m & \mathbf{0} \\ \mathbf{J}_m & \mathbf{I}_m \end{bmatrix} \begin{bmatrix} \mathbf{I}_m & -\frac{1}{2}\mathbf{J}_m \\ \mathbf{0} & \mathbf{I}_m \end{bmatrix} & (M \text{ is even}) \\ \begin{bmatrix} \mathbf{I}_m & \mathbf{0} \\ \begin{bmatrix} \mathbf{0} \\ \mathbf{J}_m \end{bmatrix} & \mathbf{I}_{m+1} \end{bmatrix} \begin{bmatrix} \mathbf{I}_m & \begin{bmatrix} \mathbf{0} & -\frac{1}{2}\mathbf{J}_m \end{bmatrix} \\ \mathbf{0} & \mathbf{I}_{m+1} \end{bmatrix} & (M \text{ is odd}) \end{cases}$$

and

$$\mathbf{W}_R = \begin{cases} \begin{bmatrix} \mathbf{I}_m & \frac{1}{2}\mathbf{J}_m \\ \mathbf{0} & \mathbf{I}_m \end{bmatrix} \begin{bmatrix} \mathbf{I}_m & \mathbf{0} \\ -\mathbf{J}_m & \mathbf{I}_m \end{bmatrix} & (M \text{ is even}) \\ \begin{bmatrix} \mathbf{I}_m & \begin{bmatrix} \mathbf{0} & \frac{1}{2}\mathbf{J}_m \end{bmatrix} \\ \mathbf{0} & \mathbf{I}_{m+1} \end{bmatrix} \begin{bmatrix} \mathbf{I}_m & \mathbf{0} \\ \begin{bmatrix} \mathbf{0} \\ -\mathbf{J}_m \end{bmatrix} & \mathbf{I}_{m+1} \end{bmatrix} & (M \text{ is odd}). \end{cases}$$

The top half of Fig. 1 outlines the building block of L-LPFB in even channel case. Let $\hat{}$ be a matrix factorized into lifting structures with rounding operations. Hence, $\hat{\mathbf{\Xi}}_k$, $\hat{\mathbf{U}}_{e,k}$, $\hat{\mathbf{V}}_{e,k}$, $\hat{\mathbf{U}}_{o,k}$, and $\hat{\mathbf{V}}_{o,k}$ respectively mean matrices factorizing $\mathbf{\Xi}_k$, $\mathbf{U}_{e,k}$, $\mathbf{V}_{e,k}$, $\mathbf{U}_{o,k}$, and $\mathbf{V}_{o,k}$ into lifting structures with rounding operations. Although any lifting factorization can be applied to them if each $|\det(\mathbf{U}_{e,k})|$, $|\det(\mathbf{V}_{e,k})|$, $|\det(\mathbf{U}_{o,k})|$, $|\det(\mathbf{V}_{o,k})|$, and $|w_k|$ is an integer value, single-row elementary reversible matrices (SERMs) [18] have been applied to PULPFBs designed in this paper because they have fewer rounding operations than the others. Also, let $\mathbf{W}_0$ be $\mathbf{W}$ in the last block $\mathbf{E}_0$. $\mathbf{W}_0$ in PULPFBs is factorized by using the traditional three steps lifting factorization of the Givens rotation matrix. On the other hand, BOLPFBs based on time-domain LTs (TDLTs) in [14] and lifting-based DCT in [31] are designed in this paper because they not only are simple but also have high coding performance. IrrSE cannot directly be applied to the L-LPFBs as explained in Sec. III-B. We will explain our solution to the problem in the next section.

III. Image Boundary Processing for L-LPFBs

Let *symmetry* be that of "each building block" unlike that of the "whole FB" in Smith and Eddins [2]. PR is satisfied by using such *symmetry* without receiving redundant signals in the synthesis bank. First, IrrSE is investigated in both case of even and odd channels. Furthermore, RevSE for the lossless mode is presented with *Cases I* and *II*. *Case I* means building blocks that do not step over the image boundary, and *Case II* means those that just step over the image boundary. Moreover, the redundancy of RevSE is eliminated by extending non-expansive convolution [13], called RevSNEC.

A. *Irreversible Symmetric Extension (IrrSE)*

Fig. 2 shows IrrSE in even channel case. Let $\mathcal{X}_k$, $\mathbf{J}_M\mathcal{X}_k$, $\mathcal{Y}_k$, and $\mathcal{Z}_k$ correspond to an $M \times 1$ input signal vector for a building block $\mathbf{\Xi}_k$, a reflected vector of $\mathcal{X}_k$, an output signal vector of $\mathbf{\Xi}_k\mathcal{X}_k$, and an output signal vector of $\mathbf{\Xi}_k\mathbf{J}_M\mathcal{X}_k$ as $\mathcal{Y}_k = \mathbf{\Xi}_k\mathcal{X}_k$ and $\mathcal{Z}_k = \mathbf{\Xi}_k\mathbf{J}_M\mathcal{X}_k$. *Symmetry* means

$$\mathcal{Y}_k = \mathbf{J}_M\mathcal{Z}_k. \tag{2}$$

We demonstrate this *symmetry* is satisfied in both *Cases I* and *II*.

1) Case I (Not Stepping Over Image Boundary): $\mathcal{X}_k$ is an input signal vector for $\mathbf{\Xi}_k$ that does not step over the image boundary in this subsection. Let $\mathcal{X}_k$ be $\mathcal{X}_k = [\mathcal{A}_k^T, \mathcal{B}_k^T]^T$ (M is even) or $[\mathcal{A}_k^T, c_k, \mathcal{B}_k^T]^T$ (M is odd) where $\mathcal{A}_k$ and $\mathcal{B}_k$ are $m \times 1$ vectors and c_k is a scalar. Also, let $\mathbf{U}_{o,k}$ (k is even) be redefined as

$$\mathbf{U}_{o,k} = \begin{bmatrix} \mathbf{u}_k & \mathbf{s}_k \\ \mathbf{t}_k & u_k \end{bmatrix}$$

where $\mathbf{u}_k$, $\mathbf{s}_k$, $\mathbf{t}_k$, and u_k correspond to $m \times m$, $m \times 1$, $1 \times m$ matrices, and a scalar. The output signal vectors $\mathcal{Y}_k$ and $\mathcal{Z}_k$ are expressed by

$$\begin{aligned} \mathcal{Y}_k &= \mathbf{\Xi}_k\mathcal{X}_k \\ &= \begin{cases} \frac{1}{2}\begin{bmatrix} \mathbf{U}_{e,k}\mathcal{U}_k + \mathbf{J}_m\mathbf{V}_{e,k}\mathcal{V}_k \\ \mathbf{J}_m\mathbf{U}_{e,k}\mathcal{U}_k - \mathbf{V}_{e,k}\mathcal{V}_k \end{bmatrix} & (M \text{ is even}) \\ \frac{1}{2}\begin{bmatrix} \mathbf{u}_k\mathcal{U}_k + \sqrt{2}c_k\mathbf{s}_k + \mathbf{J}_m\mathbf{V}_{o,k}\mathcal{V}_k \\ \sqrt{2}\mathbf{t}_k\mathcal{U}_k + 2u_kc_k \\ \mathbf{J}_m(\mathbf{u}_k\mathcal{U}_k + \sqrt{2}c_k\mathbf{s}_k) - \mathbf{V}_{o,k}\mathcal{V}_k \end{bmatrix} & \\ & (M \text{ is odd, } k \text{ is even}) \\ \frac{1}{2}\begin{bmatrix} \mathbf{U}_{o,k}\mathcal{U}_k + \mathbf{J}_m\mathbf{V}_{o,k}\mathcal{V}_k \\ w_kc_k \\ \mathbf{J}_m\mathbf{U}_{o,k}\mathcal{U}_k - \mathbf{V}_{o,k}\mathcal{V}_k \end{bmatrix} & (M \text{ is odd, } k \text{ is odd}) \end{cases} \end{aligned}$$

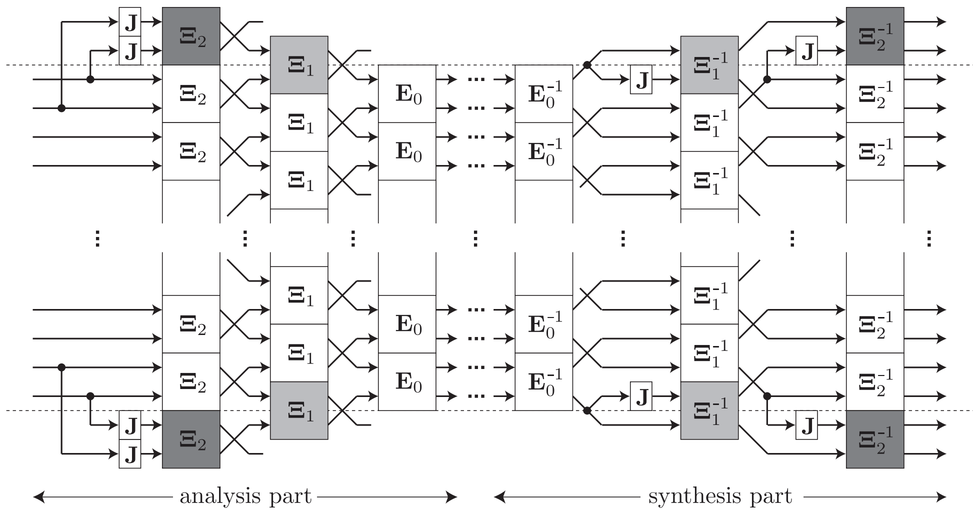

Fig. 2. IrrSE by $M \times 3M$ LPFB in even channel case (dashed lines, bold arrows, narrow arrows, dark gray blocks, light gray blocks, and white blocks correspond to image boundary, $m \times 1$ vector signals, scalar signals, blocks that do not step over image boundary, blocks that just step over image boundary, and inner blocks).

and

$$\mathcal{Z}_k = \Xi_k \mathbf{J}_M \mathcal{X}_k$$

$$= \begin{cases} \frac{1}{2}\begin{bmatrix} \mathbf{U}_{e,k}\mathcal{U}_k - \mathbf{J}_m \mathbf{V}_{e,k}\mathcal{V}_k \\ \mathbf{J}_m \mathbf{U}_{e,k}\mathcal{U}_k + \mathbf{V}_{e,k}\mathcal{V}_k \end{bmatrix} & (M \text{ is even}) \\ \frac{1}{2}\begin{bmatrix} \mathbf{u}_k\mathcal{U}_k + \sqrt{2}c_k\mathbf{s}_k - \mathbf{J}_m\mathbf{V}_{o,k}\mathcal{V}_k \\ \sqrt{2}\mathbf{t}_k\mathcal{U}_k + 2u_kc_k \\ \mathbf{J}_m(\mathbf{u}_k\mathcal{U}_k + \sqrt{2}c_k\mathbf{s}_k) + \mathbf{V}_{o,k}\mathcal{V}_k \end{bmatrix} & \\ & (M \text{ is odd, } k \text{ is even}) \\ \frac{1}{2}\begin{bmatrix} \mathbf{U}_{o,k}\mathcal{U}_k - \mathbf{J}_m \mathbf{V}_{o,k}\mathcal{V}_k \\ w_kc_k \\ \mathbf{J}_m \mathbf{U}_{o,k}\mathcal{U}_k + \mathbf{V}_{o,k}\mathcal{V}_k \end{bmatrix} & (M \text{ is odd, } k \text{ is odd}), \end{cases}$$

where $\mathcal{U}_k = \mathcal{A}_k + \mathbf{J}_m\mathcal{B}_k$ and $\mathcal{V}_k = \mathbf{J}_m\mathcal{A}_k - \mathcal{B}_k$, respectively. Consequently, it is clear that *symmetry* is satisfied as $\mathcal{Y}_k = \mathbf{J}_M\mathcal{Z}_k$ in Eq. (2). Precisely, this means that when an input signal vector is the reflected vector of another input signal vector, their output signal vectors also have the same relationship.

2) Case II (Just Stepping Over Image Boundary): $\mathcal{X}_k$ is an input signal vector for Ξ_k that just steps over the image boundary in this subsection. Let $\mathcal{X}_k$ be $\mathcal{X}_k = [(\mathbf{J}_m\mathcal{B}_k)^T, \mathcal{B}_k^T]^T$ (M is even) or $[(\mathbf{J}_m\mathcal{B}_k)^T, c_k, \mathcal{B}_k^T]^T$ (M is odd) where $\mathcal{B}_k$ is an $m \times 1$ vector and c_k is a scalar. Similar to *Case I*, it is clear that *symmetry* is satisfied as $\mathcal{Y}_k = \mathbf{J}_M\mathcal{Z}_k$ in Eq. (2) where

$$\mathcal{Y}_k = \mathcal{Z}_k = \begin{cases} \begin{bmatrix} \mathbf{U}_{e,k}\mathbf{J}_m\mathcal{B}_k \\ \mathbf{J}_m\mathbf{U}_{e,k}\mathbf{J}_m\mathcal{B}_k \end{bmatrix} & (M \text{ is even}) \\ \begin{bmatrix} \mathbf{U}_{o,k}\mathbf{J}_m\mathcal{B}_k \\ w_kc_k \\ \mathbf{J}_m\mathbf{U}_{o,k}\mathbf{J}_m\mathcal{B}_k \end{bmatrix} & (M \text{ is odd}). \end{cases}$$

B. Reversible Symmetric Extension (RevSE)

IrrSE in Sec. III-A is only for the lossy mode. We solve the problem with *symmetry* lost due to rounding errors in the lossless mode in this subsection. It can be solved with a very simple matrix manipulation where $\hat{\Xi}_k$ for extended signals is replaced with $\mathbf{J}_M\hat{\Xi}_k\mathbf{J}_M$ except for the case where the process involves just stepping over the image boundary. Fig. 3 shows a realization of the *symmetry* of L-LPFBs with rounding operations in even channel case.

1) Case I (Not Stepping Over Image Boundary): When $\mathcal{X}_k$ is an input signal vector for Ξ_k that does not step over the image boundary and rounding operations are considered, this is expressed as $\mathcal{Y}'_k \triangleq \hat{\Xi}_k\mathcal{X}_k \neq \mathcal{Y}_k$ and $\mathcal{Z}'_k \triangleq \hat{\Xi}_k\mathbf{J}_M\mathcal{X}_k \neq \mathcal{Z}_k$. Obviously, *symmetry* is lost as $\mathcal{Z}'_k \neq \mathbf{J}_M\mathcal{Y}'_k$ due to rounding error on each lifting step. Therefore, we cannot use this extension as it is. We need to refocus on Ξ_k before it is factorized into lifting structures. According to Eq. (2), Ξ_k can be represented by

$$\Xi_k = \mathbf{J}_M\Xi_k\mathbf{J}_M. \tag{3}$$

However, when $\hat{\Xi}_k$ is used instead of Ξ_k, this relationship is not preserved completely as $\hat{\Xi}_k \neq \mathbf{J}_M\hat{\Xi}_k\mathbf{J}_M$, where each building block $\hat{\Xi}_k$ for extended signals is replaced by $\mathbf{J}_M\hat{\Xi}_k\mathbf{J}_M$. Although this transform at the boundary is different from a normal transform with $\hat{\Xi}_k$, this difference is trivial. By replacing $\hat{\Xi}_k$ for extended signals, the implementation in the case of reflected input signal vector $\mathbf{J}_M\mathcal{X}_k$ is expressed as $\mathbf{J}_M\hat{\Xi}_k\mathbf{J}_M \cdot \mathbf{J}_M\mathcal{X}_k = \mathbf{J}_M\hat{\Xi}_k\mathcal{X}_k = \mathbf{J}_M\mathcal{Y}'_k$. Fig. 1 shows the *symmetry* in building blocks $\hat{\Xi}_k$ and $\mathbf{J}\hat{\Xi}_k\mathbf{J}$ of L-LPFB in even cannel case. As a result, it is clear that *symmetry* can be satisfied by a simple matrix manipulation for extended signals as Eq. (3) even if rounding operations are implemented.

2) Case II (Just Stepping Over Image Boundary): When $\mathcal{X}_k$ is an input signal vector for Ξ_k that just steps over the image boundary and rounding operations are considered, it is clear that *symmetry* as

$$\mathcal{Y}'_k = \mathbf{J}_M\mathcal{Z}'_k, \tag{4}$$

where

$$\mathcal{Y}'_k = \mathcal{Z}'_k = \begin{cases} \begin{bmatrix} \hat{\mathbf{U}}_{e,k}\mathbf{J}_m\mathcal{B}_k \\ \mathbf{J}_m\hat{\mathbf{U}}_{e,k}\mathbf{J}_m\mathcal{B}_k \end{bmatrix} & (M \text{ is even}) \\ \begin{bmatrix} \hat{\mathbf{U}}_{o,k}\mathbf{J}_m\mathcal{B}_k \\ w_kc_k \\ \mathbf{J}_m\hat{\mathbf{U}}_{o,k}\mathbf{J}_m\mathcal{B}_k \end{bmatrix} & (M \text{ is odd}), \end{cases}$$

is structurally satisfied even if the rounding operations are implemented in this case similar to those in Sec. III-A2. $\hat{\Xi}_k$ for extended signals can be replaced by $\mathbf{J}_M\hat{\Xi}_k\mathbf{J}_M$ in this case because it is clear that $\hat{\Xi}_k = \mathbf{J}_M\hat{\Xi}_k\mathbf{J}_M$ unlike that in Sec. III-B1, where we did not replace it for the sake of simplicity.

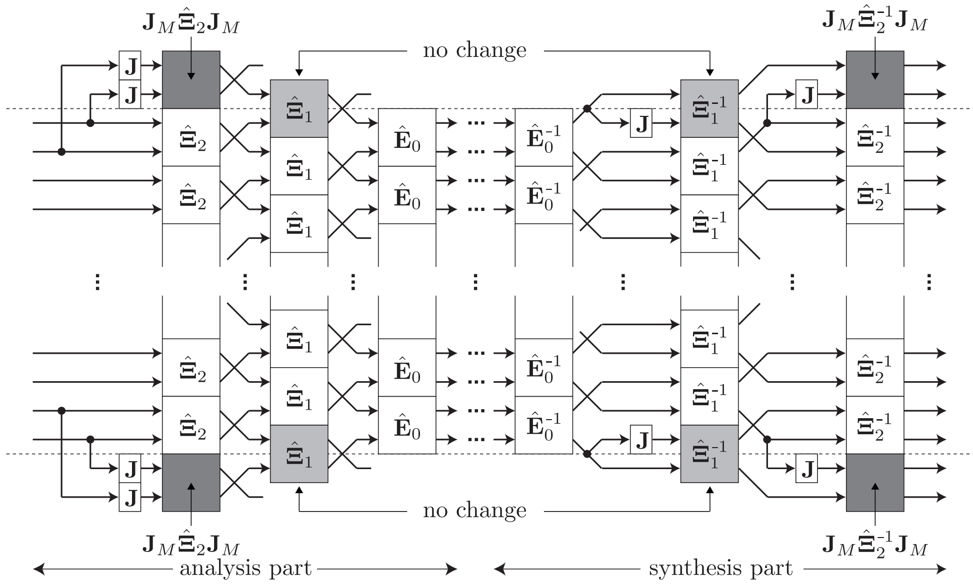

Fig. 3. RevSE by $M \times 3M$ L-LPFB in even channel case (dashed lines, bold arrows, narrow arrows, dark gray blocks, light gray blocks, and white blocks correspond to image boundary, $m \times 1$ vector signals, scalar signals, blocks that do not step over image boundary, blocks that just step over image boundary, and inner blocks).

C. Reversible Symmetric Non-Expansive Convolution (RevSNEC)

It is important for the input and output signals for $\hat{\mathbf{\Xi}}_k$ to always achieve *symmetry* as explained in Sec. III-B. Therefore, only $\hat{\mathbf{\Xi}}_k$ that just stepping over the image boundary should be considered, and only m or $m+1$ output signals are used to the next block as follows:

1) When M is even, either $\hat{\mathbf{U}}_{e,k}\mathbf{J}_m\mathcal{B}_k$ or $\mathbf{J}_m\hat{\mathbf{U}}_{e,k}\mathbf{J}_m\mathcal{B}_k$ in the output signals in Eq. (4) are used.
2) When M is odd, either $[(\hat{\mathbf{U}}_{o,k}\mathbf{J}_m\mathcal{B}_k)^T, (w_k c_k)^T]^T$ or $\mathbf{J}_m\hat{\mathbf{U}}_{o,k}\mathbf{J}_m\mathcal{B}_k$ in the output signals in Eq. (4) are used.

Consequently, RevSE in the above subsection can be replaced by non-expansive convolution [13], called RevSNEC, as seen in Fig. 4. This RevSNEC is less complex because it does not need any temporarily extensions to the input and output signals at the image boundary. Also, since $\hat{\mathbf{U}}_{e,k}$ ($k \neq 0$) usually adopts $\mathbf{I}_m$ as discussed in Sec. II-A, $\mathbf{J}_m\hat{\mathbf{U}}_{e,k}$ and $\hat{\mathbf{U}}_{e,k}\mathbf{J}_m$ are simply replaced by $\mathbf{J}_m$.

IV. Results

A. Filter Optimization

We designed 8×16 and 8×24 PULPFBs, which have $\mathbf{U}_{e,k} = \mathbf{I}_m$ ($k \neq 0$), $\mathbf{U}_{e,0}^{-1} = \mathbf{U}_{e,0}^T$ and $\mathbf{V}_{e,k}^{-1} = \mathbf{V}_{e,k}^T$, based on Sec. II-B and 8×16 and 8×24 BOLPFBs based on TDLTs in [14] and lifting-based DCT in [31]. We optimized the design parameters by using `fminunc.m` in the `Optimization ToolBox` of `MATLAB` and only coding gain C_{CG} as the cost function [1] for simple design. Moreover, since less DC leakage is one of the most important properties in FB theory for image compression, we parameterized the initial blocks of LPFBs for one degree of regularity [32].

B. Application to Lossy-to-Lossless Image Coding

The resulting LPFBs were applied to lossy-to-lossless image coding. Integer-to-integer transforms can be obtained by using a rounding operation at each lifting step. A wavelet-based coder (embedded zerotree wavelet based on intraband partitioning: EZW-IP) [33] was used in the simulation to fairly evaluate the performance of transforms. Also, RevSNEC, PE, and IrrSE were used for the image boundary processing in the designed LPFBs. We compared the lossy image coding results in Table I in the peak signal-to-noise ratio (PSNR): PSNR [dB] $= 10\log_{10}(\text{MAX}_p^2/\text{MSE})$, where MAX_p and MSE are the maximum possible pixel value of the image and the mean squared error, respectively, at 0.25, 0.50, and 1.00 bit per pixel (bpp) for several test images: 512×512 8-bit standard grayscale images, 512×768 8-bit Kodak grayscale images, and 2816×1600 16-bit clipped grayscale images in [34]. The bold numerals indicate the best PSNRs. 9/7-tap DWT (9/7-DWT) and 4×8 HLT are the transforms used in JPEG 2000 and JPEG XR lossy modes, respectively. Table I shows that most LPFBs with the RevSNEC achieves better lossy coding than the conventional methods. Fig. 5 illustrates the comparison of a particular area of the image *Barbara*. It is obvious that the proposed RevSNEC is better than PE and the boundary processing for HLT in JPEG XR in the image boundary at the right of the images in Fig. 5. Also, the LPFBs with the RevSNEC achieved almost same performance compared with the IrrSE which can achieve only lossy mode. Since the RevSNEC in 8×16 case is completely equivalent to the IrrSE in same case, Table II show the results of IrrSE only in 8×24 case.

Since the resulting LPFBs are integer-to-integer transforms, we can also obtain lossless reconstructed images at high bit rates. The performance of lossless coding at the lossless bit rate (LBR): LBR [bpp] $=$ (Total number of bits [bit])$/$(Total number of pixels [pixel]) is summarized in Table II. The bold numerals mean the best LBRs. 5/3-tap DWT (5/3-DWT) and 4×8 HLT are the transforms used in JPEG 2000 and JPEG XR lossless modes, respectively. Although the LPFBs with the RevSNEC are often inferior as compared with DWT and HLT in Kodak images and 16-bit large images, they demonstrated their effectiveness in images with high frequency components.

V. Conclusion

This paper has presented reversible symmetric extension (RevSE) for M-channel lifting-based linear-phase filter banks (L-LPFBs) applied to lossy-to-lossless image coding. Since the proposed RevSE has similar smoothness to an irreversible symmetric extension (IrrSE) at the image boundary, it does not generate distortion at the image boundary even if rounding operations are used. Moreover, complexity is lessened by extending non-expansive convolution, called reversible

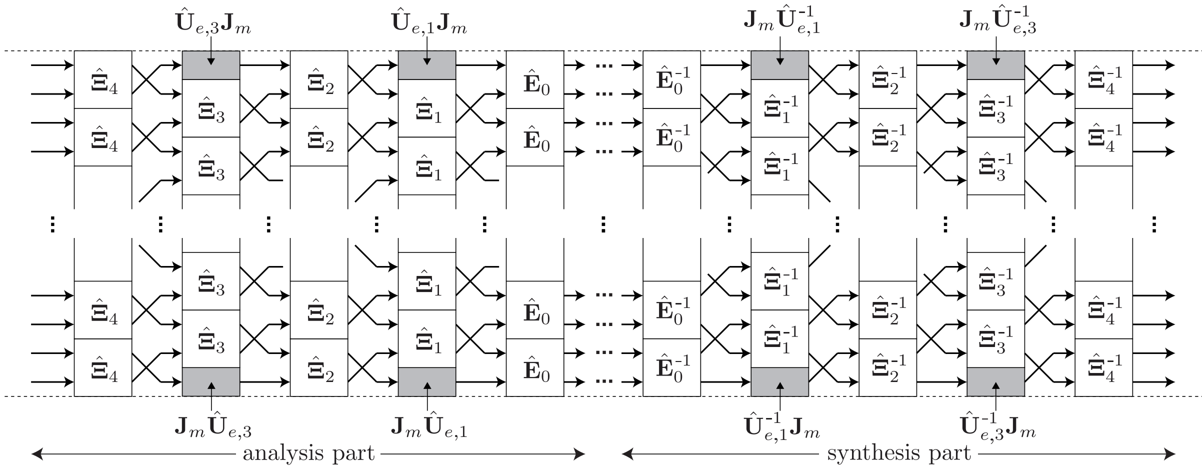

Fig. 4. RevSNEC by $M \times 5M$ L-LPFB in even channel case (dashed lines, bold arrows, narrow arrows, dark gray blocks, light gray blocks, and white blocks correspond to image boundary, $m \times 1$ vector signals, scalar signals, blocks that do not step over image boundary, blocks that just stepping over image boundary, and inner blocks).

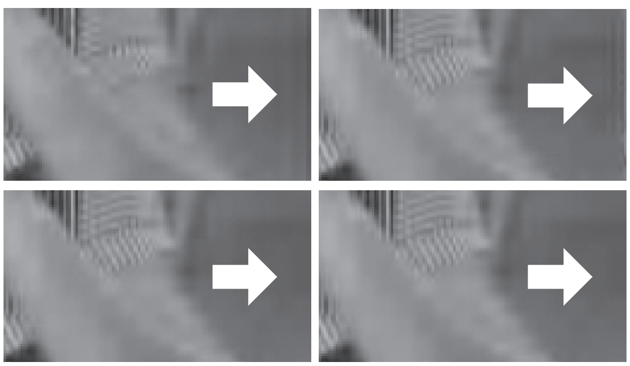

Fig. 5. Comparison of particular area of image *Barbara* reconstructed with 8×24 LPFBs when bit rate is 0.25 [bpp] (Left, top, and bottom boundaries of each image are not image boundaries.): (top-left) 4×8 HLT, (top-right) 8×24 BOLPFBs with the PE, (bottom-left) 8×24 BOLPFBs with the IrrSE, and (bottom-right) 8×24 BOLPFBs with the RevSNEC.

symmetric non-expansive convolution (RevSNEC). As a result, it achieves better performance in lossy-to-lossless image coding than periodic extension (PE).

Acknowledgment

The authors would like to thank the anonymous reviewers and Dr. S. Kyochi for providing many constructive suggestions that significantly improve the presentation of this paper. This work was supported by JSPS Grant-in-Aid for Young Scientists (B) Grant Number 25820152.

References

[1] P. P. Vaidyanathan, *Multirate Systems and Filter Banks*. Englewood Cliffs, NJ: Prentice Hall, 1992.

[2] M. J. T. Smith and S. L. Eddins, "Analysis/synthesis techniques for subband image coding," *IEEE Trans. Signal Process.*, vol. 38, no. 8, pp. 1446–1456, Aug. 1990.

[3] P. P. Vaidyanathan and T. Chen, "Role of anticausal inverses in multirate filter-banks–part II: The FIR case, factorizations, and biorthogonal lapped transforms," *IEEE Trans. Signal Process.*, vol. 43, no. 5, pp. 1103–1115, May 1995.

[4] T. D. Tran, R. L. de Queiroz, and T. Q. Nguyen, "Linear-phase perfect reconstruction filter bank: Lattice structure, design, and application in image coding," *IEEE Trans. Signal Process.*, vol. 48, no. 1, pp. 133–147, Jan. 2000.

[5] L. Gan and K.-K. Ma, "A simplified lattice factorization for linear-phase perfect reconstruction filter bank," *IEEE Signal Process. Lett.*, vol. 8, no. 7, pp. 207–209, July 2001.

[6] T. D. Tran, "M-channel linear phase perfect reconstruction filter bank with rational coefficients," *IEEE Trans. Circuits Syst. I*, vol. 49, no. 7, pp. 914–927, July 2002.

[7] Y. Tanaka, M. Ikehara, and T. Q. Nguyen, "A lattice structure of biorthogonal linear-phase filter banks with higher order feasible building blocks," *IEEE Trans. Circuits Syst. I*, vol. 55, no. 8, pp. 2322–2331, Sep. 2008.

[8] S. Muramatsu, D. Han, T. Kobayashi, and H. Kikuchi, "Directional lapped orthogonal transform: Theory and design," *IEEE Trans. Image Process.*, vol. 21, no. 5, pp. 2434–2448, May 2012.

[9] H. S. Malvar and D. H. Staelin, "The LOT: Transform coding without blocking effects," *IEEE Trans. Acoust., Speech, Signal Process.*, vol. 37, no. 4, pp. 553–559, Apr. 1989.

[10] H. S. Malvar, "Lapped transforms for efficient transform/subband coding," *IEEE Trans. Acoust., Speech, Signal Process.*, vol. 38, no. 6, pp. 969–978, June 1990.

[11] ——, *Signal Processing with Lapped Transforms*. Norwood, MA: Artech House, 1992.

[12] R. L. de Queiroz, T. Q. Nguyen, and K. R. Rao, "The GenLOT: Generalized linear-phase lapped orthogonal transform," *IEEE Trans. Signal Process.*, vol. 44, no. 3, pp. 497–507, Mar. 1996.

[13] T. Nagai, M. Ikehara, M. Kaneko, and A. Kurematsu, "Generalized unequal length lapped orthogonal transform for subband image coding," *IEEE Trans. Signal Process.*, vol. 48, no. 12, pp. 3365–3378, Dec. 2000.

[14] T. D. Tran, J. Liang, and C. Tu, "Lapped transform via time-domain pre- and post-filtering," *IEEE Trans. Signal Process.*, vol. 6, no. 6, pp. 1557–1571, June 2003.

[15] W. Sweldens, "The lifting scheme: A custom-design construction of biorthogonal wavelets," *Appl. Comput. Harmon. Anal.*, vol. 3, no. 2, pp. 186–200, Apr. 1996.

[16] ——, "The lifting scheme: A construction of second generation wavelets," *SIAM J. Math. Anal.*, vol. 29, no. 2, pp. 511–546, 1997.

[17] I. Daubechies and W. Sweldens, "Factoring wavelet transforms into lifting steps," *J. Fourier Anal. Appl.*, vol. 4, no. 3, pp. 245–267, 1998.

[18] P. Hao and Q. Shi, "Matrix factorizations for reversible integer mapping," *IEEE Trans. Signal Process.*, vol. 49, no. 10, pp. 2314–2324, Oct. 2001.

[19] Y. J. Chen and K. S. Amaratunga, "M-channel lifting factorization of perfect reconstruction filter banks and reversible M-band wavelet transforms," *IEEE Trans. Circuits Syst. II*, vol. 50, no. 12, pp. 963–976, Dec. 2003.

[20] Y. She, P. Hao, and Y. Paker, "Matrix factorizations for parallel integer transformation," *IEEE Trans. Signal Process.*, vol. 54, no. 12, pp. 4675–4684, Dec. 2006.

[21] C. M. Brislawn, "Group lifting structures for multirate filter banks I: Uniqueness of lifting factorizations," *IEEE Trans. Signal Process.*, vol. 58, no. 4, pp. 2068–2077, Apr. 2010.

[22] ——, "Group lifting structures for multirate filter banks II: Linear phase

TABLE I
LOSSY IMAGE CODING RESULTS (PSNR[dB]).

Test images	9/7-DWT [17]	4 × 8 HLT [30]	8 × 16 PULPFB RevSNEC (PE)	8 × 24 PULPFB RevSNEC (PE, IrrSE)	8 × 16 BOLPFB RevSNEC (PE)	8 × 24 BOLPFB RevSNEC (PE, IrrSE)
bit rate: 0.25 [bpp]						
Barbara	27.23	26.85	28.09 (27.97)	28.30 (28.15, 28.29)	28.42 (28.31)	**28.50** (28.34, **28.50**)
Elaine	31.50	30.81	31.27 (31.01)	31.35 (31.08, 31.35)	31.65 (31.40)	**31.66** (31.39, **31.66**)
Finger	23.49	22.96	23.63 (23.60)	23.70 (23.68, 23.70)	23.72 (23.71)	**23.72** (23.69, **23.72**)
Kodim19	28.38	27.95	28.78 (28.60)	28.87 (28.66, 28.87)	28.96 (28.78)	**29.01** (28.80, **29.01**)
Kodim20	**31.92**	31.29	30.72 (30.57)	30.77 (30.63, 30.76)	30.85 (30.76)	30.89 (30.75, 30.89)
Kodim21	27.21	26.76	27.24 (27.07)	27.28 (27.11, 27.28)	27.49 (27.37)	**27.53** (27.42, **27.53**)
Arri	33.28	33.22	33.53 (33.42)	33.71 (33.59, 33.71)	**34.09** (33.98)	34.02 (33.76, 34.02)
Face	45.96	45.49	46.27 (46.12)	46.42 (46.25, 46.42)	46.59 (46.44)	**46.63** (46.49, **46.63**)
Lake Locked	39.04	38.37	39.25 (39.10)	39.41 (39.24, 39.41)	39.71 (39.52)	**39.76** (39.57, **39.76**)
bit rate: 0.50 [bpp]						
Barbara	30.47	30.43	31.74 (31.58)	31.92 (31.73, 31.93)	32.02 (31.85)	**32.03** (31.84, **32.03**)
Elaine	32.96	32.47	33.12 (32.42)	**33.17** (32.56, **33.17**)	33.16 (32.72)	32.93 (32.61, 32.93)
Finger	25.97	25.56	26.49 (26.44)	26.53 (26.48, 26.52)	**26.79** (26.75)	26.74 (26.70, 26.74)
Kodim19	31.06	30.85	31.40 (31.23)	31.45 (31.40, 31.46)	31.60 (31.45)	**31.63** (31.48, **31.63**)
Kodim20	**35.19**	34.34	33.78 (33.69)	33.77 (33.68, 33.76)	33.98 (33.91)	34.03 (33.93, 34.03)
Kodim21	30.20	29.90	30.28 (30.15)	30.27 (30.15, 30.27)	**30.41** (30.27)	**30.41** (30.27, **30.41**)
Arri	37.30	36.75	38.05 (37.93)	38.25 (38.13, 38.25)	38.68 (38.58)	**38.78** (38.68, **38.78**)
Face	48.72	48.40	49.04 (48.95)	49.11 (49.02, 49.11)	49.24 (49.15)	**49.28** (49.19, **49.28**)
Lake Locked	42.11	41.78	42.51 (42.41)	42.67 (42.55, 42.67)	42.93 (42.82)	**43.00** (42.88, **43.00**)
bit rate:1.00 [bpp]						
Barbara	34.87	35.05	35.95 (35.77)	35.91 (35.75, 35.92)	**36.28** (36.12)	36.20 (36.02, 36.20)
Elaine	34.63	34.22	35.09 (34.87)	35.03 (34.82, 35.03)	**35.19** (35.00)	35.09 (34.89, 35.09)
Finger	29.06	29.01	30.09 (30.05)	30.13 (30.10, 30.12)	**30.58** (30.54)	30.55 (30.52, 30.55)
Kodim19	34.70	34.66	34.95 (34.80)	34.87 (34.70, 34.87)	**35.20** (35.06)	35.14 (34.99, 35.14)
Kodim20	39.45	**39.50**	38.23 (37.89)	38.08 (37.71, 38.07)	38.50 (38.27)	38.29 (38.13, 38.29)
Kodim21	34.31	34.12	34.31 (34.15)	34.22 (34.07, 34.21)	**34.46** (34.31)	34.38 (34.24, 34.31)
Arri	41.97	42.28	42.75 (42.67)	43.32 (43.01, 43.32)	43.40 (43.32)	**43.55** (43.46, **43.55**)
Face	51.68	51.47	52.05 (51.98)	52.11 (52.04, 52.11)	52.17 (52.11)	**52.20** (52.15, **52.20**)
Lake Locked	45.50	45.37	46.02 (45.95)	46.13 (46.04, 46.13)	46.32 (46.25)	**46.37** (46.30, **46.37**)

TABLE II
LOSSLESS IMAGE CODING RESULTS (LBR [BPP]).

Test images	5/3-DWT [17]	4 × 8 HLT [30]	8 × 16 PULPFB RevSNEC (PE)	8 × 24 PULPFB RevSNEC (PE)	8 × 16 BOLPFB RevSNEC (PE)	8 × 24 BOLPFB RevSNEC (PE)
Barbara	4.87	**4.81**	4.83 (4.86)	4.85 (4.88)	**4.81** (4.83)	4.83 (4.85)
Elaine	5.11	5.17	5.08 (5.12)	5.08 (5.12)	**5.07** (5.10)	5.09 (5.12)
Finger	5.84	5.71	5.70 (5.71)	**5.69** (5.70)	5.72 (5.72)	5.74 (5.75)
Kodim19	**4.90**	4.97	5.06 (5.10)	5.10 (5.13)	5.04 (5.07)	5.06 (5.09)
Kodim20	**3.85**	4.18	4.40 (4.42)	4.48 (4.51)	4.24 (4.26)	4.26 (4.28)
Kodim21	**4.96**	5.06	5.17 (5.20)	5.19 (5.22)	5.15 (5.17)	5.16 (5.19)
Arri	11.40	**11.28**	11.37 (11.39)	11.35 (11.36)	11.35 (11.37)	11.34 (11.36)
Face	10.37	10.33	10.30 (10.31)	**10.28** (10.30)	10.34 (10.35)	10.33 (10.34)
Lake Locked	11.35	11.28	11.29 (11.30)	**11.27** (11.28)	11.30 (11.31)	11.30 (11.31)

filter banks," *IEEE Trans. Signal Process.*, vol. 58, no. 4, pp. 2078–2087, Apr. 2010.

[23] T. Suzuki, M. Ikehara, and T. Q. Nguyen, "Generalized block-lifting factorization of M-channel biorthogonal filter banks for lossy-to-lossless image coding," *IEEE Trans. Image Process.*, vol. 21, no. 7, pp. 3220–3228, July 2012.

[24] W. C. Fong, S. C. Chan, A. Nallanathan, and K. L. Ho, "Integer lapped transforms and their applications to image coding," *IEEE Trans. Image Process.*, vol. 11, no. 10, pp. 1152–1159, Oct. 2002.

[25] L. Wang, J. Wu, L. Jiao, and G. Shi, "Lossy-to-lossless hyperspectral image compression based on multiplierless reversible integer TDLT/KLT," *IEEE Geosci. Remote Sens., Lett.*, vol. 6, no. 3, pp. 587–591, July 2009.

[26] T. Suzuki and M. Ikehara, "Integer fast lapped transforms based on direct-lifting of DCTs for lossy-to-lossless image coding," *EURASIP J. Image. Video Process.*, vol. 2013, no. 65, pp. 1–9, Dec. 2013.

[27] A. Skodras, C. Christopoulis, and T. Ebrahimi, "The JPEG2000 still image compression standard," *IEEE Signal Process. Mag.*, vol. 18, no. 5, pp. 36–58, Sep. 2001.

[28] F. Dufaux, G. J. Sullivan, and T. Ebrahimi, "The JPEG XR image coding standard," *IEEE Signal Process. Mag.*, vol. 26, no. 6, pp. 195–199, 204, Nov. 2009.

[29] M. D. Adams and R. K. Ward, "Symmetric-extension-compatible reversible integer-to-integer wavelet transforms," *IEEE Trans. Signal Process.*, vol. 51, no. 10, pp. 2624–2636, Oct. 2003.

[30] C. Tu, S. Srinivasan, G. J. Sullivan, S. Regunathan, and H. S. Malvar, "Low-complexity hierarchical lapped transform for lossy-to-lossless image coding in JPEG XR/HD Photo," in *Proc. of SPIE 7073*, San Diego, CA, Aug. 2008.

[31] T. Suzuki and H. Aso, "M-channel fast Hartley transform based integer DCT for lossy-to-lossless image coding," *IEICE Trans. Fundamentals.*, vol. E96-A, no. 4, pp. 762–768, Apr. 2013.

[32] T. Uto, T. Oka, and M. Ikehara, "M-channel nonlinear phase filter banks in image compression: Structure, design, and signal extension," *IEEE Trans. Signal Process.*, vol. 55, no. 4, pp. 1339–1351, Apr. 2007.

[33] Z. Liu and L. J. Karam, "An efficient embedded zerotree wavelet image codec based on intraband partitioning," in *Proc. of ICIP'00*, Vancouver, British Columbia, Canada, Sep. 2000.

[34] S. Andriani, H. Brendel, T. Seybold, and J. Goldstone, "Beyond the Kodak image set: A new reference set of color image sequences," in *Proc. of ICIP'13*, Melbourne, Australia, Sep. 2013, pp. 2289–2293.